

On the lack of influence of contact area on the solid-liquid lateral retention force

Rafael de la Madrid,^{*} Caleb Gregory, Huy Luong,[†] Tyler Stuck

Department of Physics, Lamar University, Beaumont, TX 77710

June 14, 2023

Abstract

We experimentally show that, unlike the solid-solid frictional force, the solid-liquid retention force is determined by interactions at the triple line rather than over the solid-liquid contact area, as predicted by theory. We have prepared drops whose triple line enclosed a uniform surface, a hydrophobic island, and topographical inhomogeneities, and measured the same retention force for all three cases. We have also studied the retention force on drops whose initial triple line was non-circumferential and measured different retention forces for different shapes, also as predicted by theory. The experiments with non-circumferential drops provide (1) another way to show that the retention force is not proportional to the contact area, and (2) a manner to falsify a recent theory on drop depinning.

Keywords: Wetting; dewetting; adhesion; lateral retention force.

1 Introduction

Amontons' laws of friction state that the frictional force f between two solid surfaces is proportional to the normal force (load) F_N and is independent of the apparent contact area, $f = \mu F_N$, where μ is the friction coefficient [1]. Amontons' laws, which hold under quite general conditions, seem to contradict the expectation that the frictional force should be proportional to the contact area.

One of the main insights of the modern theory of friction [2, 3] is that the frictional force is independent of the normal force and is in fact proportional to the actual contact area between the surfaces. This actual contact area arises from the points of actual

^{*}E-mail: rafael.delamadrid@lamar.edu

[†]Current address: Johnson Controls, Port Arthur, TX 77640

contact between the surfaces, and it is much smaller than the apparent contact area. For rough surfaces, the actual contact area is proportional to the normal force, and therefore for rough surfaces the frictional force is also proportional to the normal force, in agreement with Amontons' laws [2, 3].

When a drop is trying to move on a solid surface, it experiences a force that opposes motion, called the lateral retention force, f_{\parallel} , that is the solid-liquid analog of solid-solid friction. Because the liquid can deform, it seems natural to assume that the true contact area between the liquid and the solid is the same as the apparent contact area, and therefore one may be tempted to conclude that the lateral retention force is proportional to the solid-liquid contact area, as suggested in Ref. [4].

The most widely accepted expression for the lateral retention force is given by [5–9]

$$f_{\parallel} = \gamma \oint_C \cos \theta \hat{n} \cdot \hat{r} ds, \quad (1)$$

where γ is the liquid-vapor surface tension, C denotes the triple line, θ is the (varying) contact angle along the triple line, \hat{n} is a unit vector perpendicular to the triple line, and \hat{r} is a unit vector in the direction of the overall motion of the drop.

A feature of Eq. (1) that has not been highlighted in the literature is the fact that f_{\parallel} is independent of the properties of the actual solid-liquid contact area, contrary to the naive expectation that f_{\parallel} is proportional to such area [4]. What is more, if we changed the chemical or topographical properties of the contact area enclosed by the triple line, Eq. (1) predicts that f_{\parallel} remains unchanged as long as the contact angles remain unchanged. But, do contact angles remain unchanged when the properties of the contact area change?

For homogeneous surfaces, it has long been accepted that the contact angles are not affected by the contact area (see, for example, Refs. [5, 10]). For heterogeneous surfaces, the pioneering studies of Wenzel [11] and Cassie and Baxter [12] seemingly established that contact angles are affected by the properties of the contact area enclosed by the triple line. However, a few studies [13–16] have shown that contact angles depend only on interactions at the triple line and are unaffected by the properties contact area (see Ref. [17] for a review on the debate on the dependence of contact angles on the triple line vs. the solid-liquid contact area). Although in 2007 the minority view was that contact angles are unaffected by the contact area [15], it seems that nowadays that has become the majority view [18].

If the contact angles are unaffected by changes in the contact area enclosed by the triple line, Eq. (1) predicts that f_{\parallel} is also unaffected by those changes. Our first goal is to provide experimental evidence that such is the case. Essentially, we will set up experiments that are similar to those in Refs. [13–16], but we will subject the drop to an external centrifugal force and measure the force f_{\parallel} necessary to move the drop. We will show that at the onset of motion, the lateral retention force is the same whether the contact area is uniform, has a hydrophobic island, or has topographical defects.

It is well known that Eq. (1) predicts that f_{\parallel} depends on the shape of the triple

line. However, save for some exceptions (see Refs. [19–21]), experimental studies of the retention force usually deal with drops whose initial triple line has a circumferential shape [22–28]. Our second goal is to experimentally show that different shapes of the triple line will in general lead to different retention forces, as predicted by Eq. (1) and in agreement with the experimental results of Refs. [19–21]. We will prepare drops that are elongated along the parallel and perpendicular directions to the centrifugal force and show that their retention force is different from drops whose initial triple line is circumferential. The study of non-circumferential triple lines will provide additional evidence that f_{\parallel} cannot be proportional to the solid-liquid contact area.

When a drop is deposited at a given spot on a uniform, flat surface, its triple line has a circumferential shape. When an external (e.g., centrifugal) force parallel to the surface is applied on it, the drop starts leaning in the direction of the force. Typically, as the external force increases, the receding edge remains pinned to the surface, the advancing edge crawls forward, the drop spreads and, at the onset of motion, the shape of the triple line somewhat resembles the egg of a hen. When the drop moves at low speeds (or, more precisely, when the capillary number is small), the shape of the triple line becomes “quasi-rectangular” [29, 30]. As the speed increases, the drop develops a tail that eventually breaks up into small droplets [31]. Equation (1) does not describe this equilibrium-to-motion transition, an additional theoretical input is needed to describe it. A recent theory [32] describes some aspects of this transition. Specifically, the theory of Ref. [32] asserts that, in the equilibrium-to-motion transition, as the drop depins itself from the surface to start moving, the advancing edge will always move before the receding edge. Our third goal is to show that our experiments with non-circumferential drops contradict the theory of Ref. [32] but are in agreement with the experiments of Ref. [20].

Experimental verification of the consequences of Eq. (1) is important not just for its own sake, but also because Eq. (1) is not universally accepted as the correct expression for the lateral retention force [4, 33, 34]. Our hope is that the straightforward nature of our experiments will dispel any doubts [4, 33, 34] about the validity Eq. (1).

2 Experimental Section

Our experimental apparatus is the same as in Ref. [28], see Fig. 1. It consists of a metallic frame with dimensions 90 cm \times 90 cm \times 120 cm inside of which the rotary unit is mounted. The four legs of the frame are bolted to the floor to reduce mechanical vibrations. The rotary unit consists of a servo motor, a shaft, and two pairs of aluminum rails that are attached perpendicularly to the shaft. The motor is connected to a power supply and a computer, whose software controls the motor.

A metallic box is mounted on the aluminum rails. The box has two cameras placed on top and on the side, which provide top and side views of the drops. An LED panel mounted on one side of the box is used to set a common starting time in the videos of

the cameras. On the door of the metallic box, we mounted a poly methyl methacrylate (PMMA) sheet (Optix, by Plaskolite) such that, when a drop is placed on the sheet and the door is closed, the cameras have side and top views of the drop. Illumination for the side camera is provided by the outside LED panel. Lighting for the top camera is provided by a second LED panel and an optical gradient [31]. The still frames of the videos of the side (top) camera were fed into ImageJ [35] to measure the contact angles (contact area and width) of the drops. We used a syringe from Hamilton to deposit 60- μL drops of (distilled) water on the PMMA sheets. The large volume of the drops allowed us to build drops whose initial triple line had a non-circumferential shape.

Figure 2 shows the different surfaces and shapes of triple lines used in this work. Figure 2(a) represents the circumferential triple line of a drop resting on a uniform PMMA surface. Such circumferential triple line was obtained by slowly depositing the liquid on the same spot of the surface. We will refer to this kind of surface as “uniform” and this kind of triple line as “circular.” Figure 2(b) represents a PMMA surface that has a small hydrophobic island encircled by the triple line, hence the name “island.” The hydrophobic island was obtained with Fusso Coat [36]. In the “island” case, as we deposited the liquid on the center of the hydrophobic “island,” the contact area of the drop increased, and eventually the triple line moved into the PMMA surface and encircled the hydrophobic “island” completely. Figure 2(c) represents a hydrophobic surface obtained by covering the whole PMMA surface with Fusso Coat, hence the name “hydrophobic.” When we deposited the liquid at the same point on this hydrophobic surface, we obtained a circumferential triple line, but with a smaller diameter than in the “uniform” and “island” cases. Figure 2(d) represents a PMMA surface with a 5-mm-diameter circular scratch etched with a laser cutter. We will refer to this type of surface as “single.” When a 60 μL drop was deposited at the center of the circular scratch, the triple line eventually moved past the scratch and formed a circle of larger diameter than the scratch. The surfaces in Figs. 2(e) and 2(f) are essentially the same as in Fig. 2(d), but with the addition of a 3-mm-diameter (in Figure 2(e)) and a 1-mm-diameter (in Figure 2(f)) circular scratch. We will refer to those surfaces as “double” and “triple.”

On a uniform surface, besides the circular shape of Fig. 2(a), we built two other types of triple line that have elongated shapes, along the perpendicular (“tangential”) and parallel (“radial”) directions to the centrifugal force, see Figs. 2(g) and (h). The direction of the centrifugal force is represented by the arrow in Fig. 2(i). Those elongated drops were built by depositing two small, 25 μL droplets close to each other. As the two droplets grew, they eventually merged into a single drop. At the moment of the merge, the single drop had an elongated, “quasi-elliptical” shape. To keep the elongated shape, the remaining liquid in the syringe was deposited at the ends of the “major axis” of the “quasi-ellipse.”

The solid lines in Figs. 2(a)-(h) represent the initial shapes of the triple line. When the centrifugal force starts acting on the drops, those initial shapes start changing. For shapes (a)-(g), the advancing edge starts moving first as the drop spreads (expands),

whereas the receding edge remains pinned at the surface. The onset of the motion is characterized by the instant when the receding edge starts moving. However, for the “radial” shape of Fig. 2(h), the advancing edge remains pinned to the surface, and the receding edge starts moving first as the drop contracts. The onset of the motion for “radial” drops is therefore determined by the instant when the advancing edge starts moving.

The edge that determines the onset of the overall motion of the drop always goes through a stick-slip transition from rest to motion. There is therefore some ambiguity on when the actual onset of the motion occurs. Our criterion to determine the onset of the motion was that the edge that determines it had to move at the most three pixels ($69 \mu\text{m}$). We chose such criterion because after the edge we were monitoring had moved three pixels, the stick-slip transition was basically over. In some cases, the stick-slip transition was over after the edge moved two or even just one pixel, and in such cases we used motion of two or one pixel as the criterion to establish the onset of the motion. A three-pixel ($69 \mu\text{m}$) displacement is invisible to the naked eye, and we used the custom software of Ref. [28] to determine the instant at which the onset of the motion occurred. From such instant, we calculated the centrifugal force at the onset of motion, and from the centrifugal force we obtained the (maximum) lateral retention force.

To accumulate enough statistics, for each case in Fig. 2 we prepared 15 different surfaces and did three runs on each surface. Hence, the data for each case arises from about 45 runs. All the errors quoted in this paper are statistical.

Although the exact integral expression of Eq. (1) has been used in theoretical studies of the retention force [5–9], in practical applications [19–26] the variation of the contact angle along the triple line is usually not known, and one approximates the three dimensional drop by a two dimensional film. The triple line is then reduced to the advancing and receding edges, and the exact integral expression of f_{\parallel} is replaced by the following effective expression [6, 29]:

$$f_{\parallel} = k\gamma w (\cos \theta_r - \cos \theta_a), \quad (2)$$

where the shape factor k is a fudge factor that accounts for the unknown variation of θ . In practice, one measures the retention force, the width, and the advancing and receding contact angles, whereas the shape factor is calculated as $k = f_{\parallel}/w(\cos \theta_r - \cos \theta_a)$. Therefore, we will be able to explain our experimental results in terms of Eq. (2), but we will not be able to fully describe them using Eq. (1) due to our inability to measure the contact angle along the triple line.

3 Results and Discussion

3.1 First Experiment

We first measured the lateral retention forces on the “uniform,” “island,” and “hydrophobic” surfaces of Figs. 2(a)-(c).

Type	f_{\parallel} (μN)	A_0 (mm^2)	A (mm^2)	θ_a ($^\circ$)	θ_r ($^\circ$)	w (mm)	k
Uniform	183 ± 4	48.6 ± 0.2	49.8 ± 0.2	69.9 ± 0.3	47.2 ± 0.7	7.79 ± 0.02	0.97 ± 0.04
Island	184 ± 5	48.1 ± 0.3	50.6 ± 0.2	69.2 ± 0.4	46.4 ± 0.6	7.78 ± 0.02	0.98 ± 0.04
Hydrophobic	116 ± 5	29.4 ± 0.3	30.2 ± 0.1	101.5 ± 0.6	85.6 ± 0.6	6.01 ± 0.02	0.97 ± 0.07

Table 1: Experimental data of “uniform,” “island,” and “hydrophobic” surfaces.

Table 1 displays the magnitude of the lateral retention force f_{\parallel} , the initial (A_0) and final (A) contact areas, the advancing (θ_a) and receding (θ_r) contact angles, the width w of the drop at the onset of the motion, and the shape factor k .

As can be seen in Table 1, the retention forces of the “uniform” and “island” cases are roughly the same. Hence, the onset of the motion of the drop is not affected by the hydrophobic island. However, in the “hydrophobic” case, the triple line sits on the hydrophobic coating and f_{\parallel} decreases dramatically. Thus, we conclude that f_{\parallel} is not influenced by the hydrophobic island, and is affected only when the triple line interacts with the hydrophobic coating. We can also see in Table 1 that the other wetting parameters (contact area, contact angles and width) are roughly the same in the “uniform” and “island” cases, but they change in the “hydrophobic” case, and therefore are affected by interactions at the triple line rather than over the contact area. Hence, Eqs. (1) and (2) are consistent with our experimental finding that f_{\parallel} is the same in the “uniform” and “island” cases, but changes in the “hydrophobic” one. Interestingly, the shape factor of the “hydrophobic” case is very similar to those of the “uniform” and “island” cases, even though the other wetting parameters are very different.

3.2 Second Experiment

In a second experiment, we compared the lateral retention forces on drops deposited on the “uniform,” “single,” “double,” and “triple” surfaces of Fig. 2, see data in Table 2.

The solid-solid frictional force certainly increases as the roughness of the contact area increases. However, similar to our first experiment, the retention force seems to be unaffected by the rough scratches contained within the triple line, and has essentially the same value as we increase the number of circular scratches from none (“uniform”) to three (“triple”). As long as the triple line doesn’t touch the scratches, the motion of the drop remains unaffected by them. However, after the motion of the drop starts,

Type	f_{\parallel} (μN)	A_0 (mm^2)	A (mm^2)	$\theta_a^{(\circ)}$	$\theta_r^{(\circ)}$	w (mm)	k
Uniform	187 ± 3	48.6 ± 0.1	50.8 ± 0.1	67.5 ± 0.4	43.8 ± 0.7	7.82 ± 0.02	0.98 ± 0.04
Single	182 ± 3	48.1 ± 0.3	50.4 ± 0.3	69.4 ± 0.5	46.4 ± 0.7	7.75 ± 0.04	0.97 ± 0.04
Double	189 ± 4	48.5 ± 0.2	50.9 ± 0.2	68.9 ± 0.3	44.1 ± 0.4	7.76 ± 0.02	0.94 ± 0.03
Triple	180 ± 5	47.9 ± 0.2	49.7 ± 0.2	69.5 ± 0.4	46.1 ± 0.5	7.71 ± 0.03	0.94 ± 0.04

Table 2: Experimental data of “uniform,” “single,” “double,” and “triple” surfaces.

the triple line eventually reaches the outer circular scratch, and the receding edge gets pinned to the scratch. A centrifugal force of about $330 \mu\text{N}$ is then necessary to depin the drop from the scratch. The pinning at the scratch is so strong that in many runs the drop breaks up and the tail of the drop stays at the scratch while the rest of the drop moves away. Thus, even though the drop is firmly pinned to the scratches when the triple line reaches them, its motion is unaffected when the scratches are contained within the triple line.

As can be seen in Table 2, the contact angles, width and shape factor are essentially the same for all four types of surface roughness, and therefore Eq. (1) and (2) are consistent with our experimental findings.

3.3 Third Experiment

In the third experiment, we studied the influence of the shape of the triple line on the retention force, by comparing the retention force of “circular,” “tangential,” and “radial” drops on uniform PMMA surfaces, see Fig. 2. Table 3 displays the data of the third experiment.

Type	f_{\parallel} (μN)	A_0 (mm^2)	A (mm^2)	$\theta_a^{(\circ)}$	$\theta_r^{(\circ)}$	w (mm)	k
Circular	187 ± 3	48.6 ± 0.1	50.8 ± 0.1	67.5 ± 0.4	43.8 ± 0.7	7.82 ± 0.02	0.98 ± 0.04
Radial	169 ± 2	52.9 ± 0.3	50.6 ± 0.1	68.4 ± 0.3	44.5 ± 0.5	6.93 ± 0.03	0.98 ± 0.02
Tangential	215 ± 3	53.2 ± 0.2	53.9 ± 0.4	69.1 ± 0.2	46.8 ± 0.4	9.46 ± 0.05	0.97 ± 0.03

Table 3: Experimental data of drops with “circular,” “radial” and “tangential” triple-line shapes.

Contrary to solid-solid friction, the shape of the solid-liquid contact area affects f_{\parallel} . The retention force for “tangential” drops is larger than for “circular” drops, which in turn is larger than for “radial” drops. Equation (2) allows us to understand this result. Because the advancing and receding contact angles and the shape factor are very similar for the three shapes in this third experiment, what basically determines f_{\parallel} is the width of the drop—the longer the width, the larger the retention force. Because $w_{\text{tangential}} > w_{\text{circular}} > w_{\text{radial}}$, it makes sense that the corresponding retention forces follow the same order.

As can be seen in Tables 1, 2 and 3, except for “radial” drops, the contact area at the onset of the motion is always larger than the initial one, that is, the drops spread before moving. Hence, as the retention force increases up to its maximum value, the contact area also increases up to its maximum value, and one may think that the size of the contact area may somehow affect the retention force, even though the roughness and the chemical composition of the contact area do not affect it. However, for “radial” drops the contact area at the onset of motion is *smaller* than the initial one, see Table 3. The reason is that for “radial” drops, as the centrifugal drop increases, the advancing edge remains pinned to the surface and the receding edge crawls forward, making the contact area decrease. Hence, if the size of the contact area was an essential factor affecting the lateral retention force, the contact area of “radial” drops should also increase as the external centrifugal force increases. However, for “radial” drops the opposite occurs.

As mentioned in the Introduction, Eq. (1) does not describe the changes that a drop experiences in the equilibrium-to-motion transition, an additional theory is needed. Recently, a theory to describe such transition was proposed in Ref. [32]. According to that theory, protrusion of the solid surface at the triple line always makes the advancing edge of the drop move *before* the receding edge does. However, our results for “radial” drops, in agreement with the results of Ref. [20], show that the theory of Ref. [32] is not correct, because for “radial” drops the advancing edge moves *after* the receding edge.

4 Conclusions

We have presented three experiments that show that the lateral retention force is determined by the interactions at the triple line and by the shape of the triple line itself, and seems to be unaffected by the properties of the contact area enclosed by the triple line, in contrast to the solid-solid frictional force, which depends on the size and roughness of the actual contact area but does not depend of the shape of its perimeter. If interactions over the contact area do affect f_{\parallel} , their influence is much smaller than the influence of the interactions at the triple line. From a theoretical point of view, our experiments are a straightforward consequence of Eq. (1), which provides an expression for the lateral retention force that depends only on quantities defined at the triple line and is unaffected by the contact area.

As expected [15], we have found that the advancing and receding contact angles are independent of the initial shape of the triple line, and of the chemical and topographical properties of the contact area. Somewhat unexpectedly, we have found that the shape factor is very similar in all cases, even for different shapes of the triple line.

Our results are consistent with, and expand the results of Refs. [13–16, 20, 21], but they are in disagreement with some of the conclusions of Refs. [4, 32–34]. In particular, our experiments with non-circumferential triple lines are in disagreement with the

theory of Ref. [32] on drop depinning.

Finally, we would like to note that, although wetting quantities such as contact angles and retention forces depend only on interactions at the triple line, some energy quantities do depend on contact area. Specifically, the energies per unit of contact area to expand, contract, slide or detach a drop are constant, and do not depend on the shape of the triple line [30].

CRediT authorship contribution statement

Rafael de la Madrid: Conceptualization, data acquisition, writing-review & editing. Caleb Gregory: Data analysis. Huy Luong: Design and construction of experimental apparatus. Tyler Stuck: Data analysis.

Acknowledgments

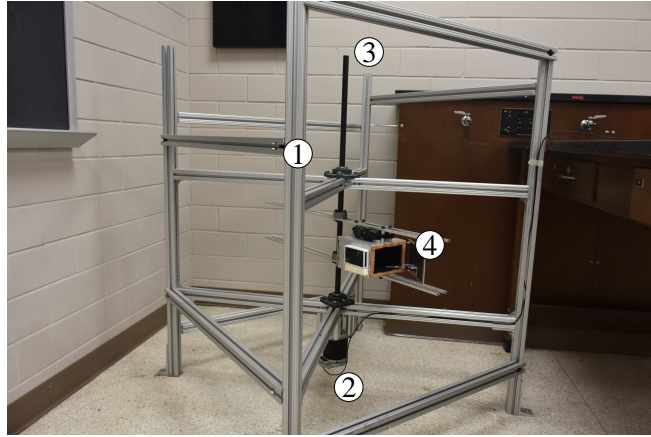
Financial support from Lamar COAS and SURF fellowships is gratefully acknowledged.

References

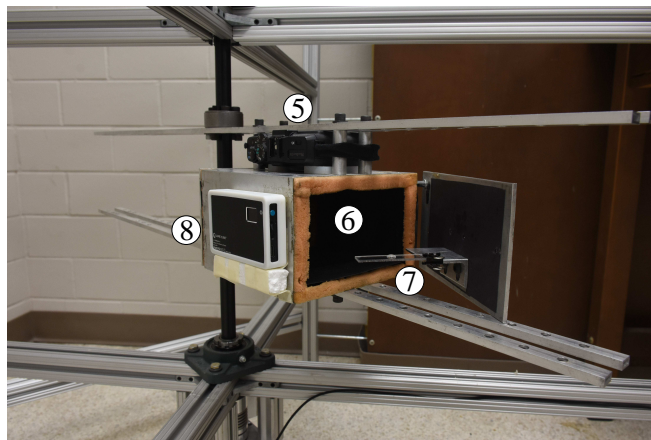
- [1] J.N. Israelachvili, *Intermolecular and Surface Forces*, Elsevier (2011).
- [2] G. Hähner, N. Spencer, *Rubbing and Scrubbing*, Phys. Today **51**, 22-27 (1998).
- [3] F.P. Bowden, D. Tabor, *The Friction and Lubrication of Solids*, Clarendon Press, Oxford (1985).
- [4] R. Tadmor, *Open Problems in Wetting Phenomena: Pinning Retention Forces*, Langmuir **37**, 6357-6372 (2021).
- [5] R.A. Brown, F.M. Orr, L.E. Scriven, *Static Drop on an Inclined Plate: Analysis by the Finite Element Method*, J. Coll. Int. Sci. **73**, 76-87 (1980).
- [6] E.B. Dussan, R.T.-P. Chow, *On the Ability of Drops or Bubbles to Stick to Non-Horizontal Surfaces of Solids*, J. Fl. Mech. **137**, 1-29 (1983).
- [7] C. Antonini, F.J. Carmona, E. Pierce, M. Marengo, A. Amirfazli, *General Methodology for Evaluating the Adhesion Force of Drops and Bubbles on Solid Surfaces*, Langmuir **25**, 6143-6154 (2009).
- [8] J. De Coninck, J.C. Fernandez Toledano, F. Dunlop, T. Huillet, *Pinning of a Drop by a Junction on an Incline*, Phys. Rev. E **96**, 042804 (2017).

- [9] F. Dunlop, A.H. Fatollahi, M. Hajirahimi, T. Huillet, *Identities for droplets with circular footprint on tilted surfaces*, R. Soc. Open Sci. **7**, 201534 (2020).
- [10] E. Rio, A. Daerr, B. Andreotti, L. Limat, *Boundary Conditions in the Vicinity of a Dynamic Contact Line: Experimental Investigation of Viscous Drops Sliding Down an Inclined Plane*, Phys. Rev. Lett. **94** 024503 (2005).
- [11] R.N. Wenzel, *Resistance of Solid Surfaces to Wetting by Water*, Ind. Eng. Chem. **28**, 988-994 (1936).
- [12] A.B.D. Cassie, S. Baxter, *Wettability of Porous Surfaces*, Trans. Faraday Soc. **40**, 546-551 (1944).
- [13] F.E. Bartell, J.W. Shepard, *Surface Roughness as Related to Hysteresis of Contact Angles. II. The Systems Paraffin-3 Molar Calcium Chloride Solution-Air and Paraffin-Glycerol-Air*, J. Phys. Chem. **57**, 455-458 (1953).
- [14] C.W. Extrand, *Contact Angles and Hysteresis on Surfaces with Chemically Heterogeneous Islands*, Langmuir **19**, 3793-3796 (2003).
- [15] L. Gao, T.J. McCarthy, *How Wenzel and Cassie Were Wrong*, Langmuir **23**, 3762-3765 (2007).
- [16] C. W. Extrand, *Origins of Wetting*, Langmuir **32**, 7697-7706 (2016).
- [17] H.Y. Erbil, *The Debate on the Dependence of Apparent Contact Angles on Drop Contact Area or Three-Phase Contact Line: A Review*, Surf. Sci. Rep. **69**, 325-365 (2014).
- [18] H.Y. Erbil, *Dependency of Contact Angles on Three-Phase Contact Line: A Review*, Colloids Interfaces **5**, 8 (2021).
- [19] R. de la Madrid, T. Whitehead, G. Irwin, *Comparison of the Lateral Retention Forces on Sessile and Pendant Water Drops on a Solid Surface*, Am. J. Phys. **83**, 531-538 (2015).
- [20] N. Janardan, M.V. Panchagnula, *Onset of Sliding Motion in Sessile Drops with Initially Non-Circular Contact Lines*, Colloids and Surfaces A: Physicochem. Eng. Aspects **498**, 146-155 (2016).
- [21] I. Ríos-López, S. Evgenidis, M. Kostoglou, X. Zabulis, T.D. Karapantsios, *Effect of Initial Droplet Shape on the Tangential Force Required for Spreading and Sliding Along a Solid Surface*, Colloids and Surfaces A: Physicochem. Eng. Aspects **549**, 164-173 (2018).
- [22] C.W. Extrand, A.N. Gent, *Retention of Liquid Drops by Solid Surfaces*, J. Coll. Int. Sci. **138**, 431-442 (1990).

- [23] A. Carre, M.E.R. Shanahan, *Drop Motion on an Inclined Plane and Evaluation of Hydrophobic Treatments to Glass*, J. Adhesion **49**, 177-185 (1995).
- [24] A.I. ElSherbini, A.M. Jacobi, *Liquid Drops on Vertical and Inclined Surfaces; I. An Experimental Study of Drop Geometry*, J. Coll. Int. Sci. **273**, 556-565 (2004).
- [25] N. Janardan, M.V. Panchagnula, *Effect of the Initial Conditions on the Onset of Motion in Sessile Drops on Tilted Plates*, Colloids and Surfaces A: Physicochem. Eng. Aspects **456**, 238-245 (2014).
- [26] P. Evgenidis, K. Kalić, M. Kostoglou, T.D. Karapantsios, *Kerberos: A Three Camera Headed Centrifugal/Tilting Device for Studying Wetting/Dewetting under the Influence of Controlled Forces*, Colloids and Surfaces A: Physicochem. Eng. Aspects **521** 38-48 (2017).
- [27] M. Jamali, H.V. Tafreshi, B. Poourdeyhimi, *Droplet Mobility on Hydrophobic Fibrous Coatings Comprising Orthogonal Fibers*, Langmuir **34**, 12488-124991 (2018).
- [28] R. de la Madrid, F. Garza, J. Kirk, H. Luong, L. Snowden, J. Taylor, B. Vizena, *Comparison of the Lateral Retention Forces on Sessile, Pendant, and Inverted Sessile Drops*, Langmuir **35**, 2871-2877 (2019).
- [29] C.G.L. Furmidge, *Studies at Phase Interfaces. I. The Sliding of Liquid Drops on Solid Surfaces and a Theory for Spray Retention*, J. Coll. Int. Sci. **17**, 309-324 (1962).
- [30] R. de la Madrid, H. Luong, J. Zumwalt, *New Insights into the Capillary Retention Force and the Work of Adhesion*, Colloids and Surfaces A: Physicochem. Eng. Aspects **637**, 128195 (2022).
- [31] T. Podgorski, J.-M. Flesselles, L. Limat, *Corners, Cusps and Pearls in Running Drops*. *Phys. Rev. Lett.* **87**, 036102 (2001).
- [32] A.K. Jena, Y.V.R. Bhimavarapu, S. Tang, J. Liu, R. Das, S. Gulec, A. Vinod, C.-W. Yao, T. Cai, R. Tadmor, *Stages that Lead to Drop Depinning and Onset of Motion*, Langmuir **38**, 92-99 (2022).
- [33] R. Tadmor, *Misconceptions in Wetting Phenomena*, Langmuir **29**, 15474-15475 (2013).
- [34] W. Xu, J. Xu, X. Li, Y. Tian, C.-H. Choi, E.-H. Yang, *Lateral Actuation of an Organic Droplet on Conjugated Polymer Electrodes Via Imbalanced Interfacial Tensions*, Soft Matter **12** 6902-6909 (2016).
- [35] <https://imagej.nih.gov/ij/>
- [36] <https://www.soft99.co.jp/en/products/detail/00298/>



(a)



(b)

Figure 1: (a) Drop centrifuge: **1**-aluminum frame; **2**-motor; **3**-shaft; **4**-box. (b) Box: **5**-top camera; **6**-side camera; **7**-PMMA sheet with drop; **8**-LED panel. Inside the box (not shown in the picture) there is a second LED panel that provides the necessary illumination for the top camera.

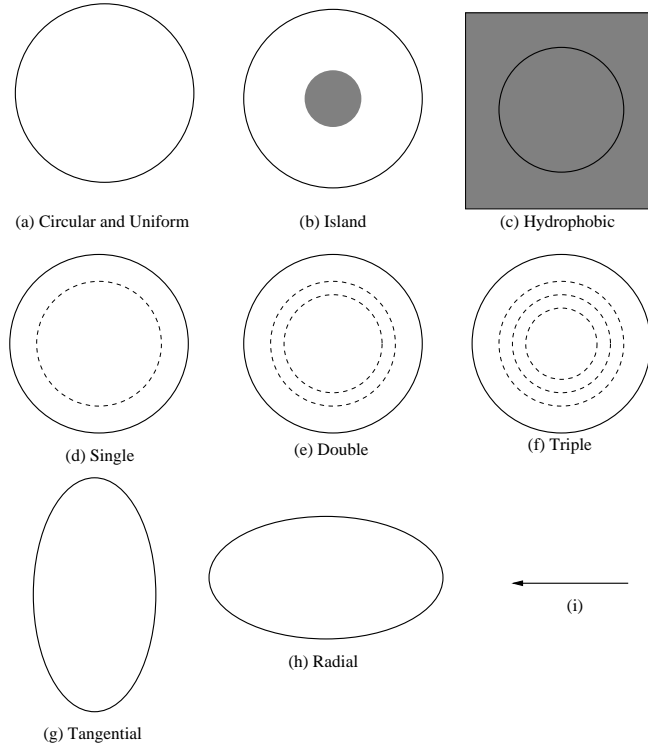
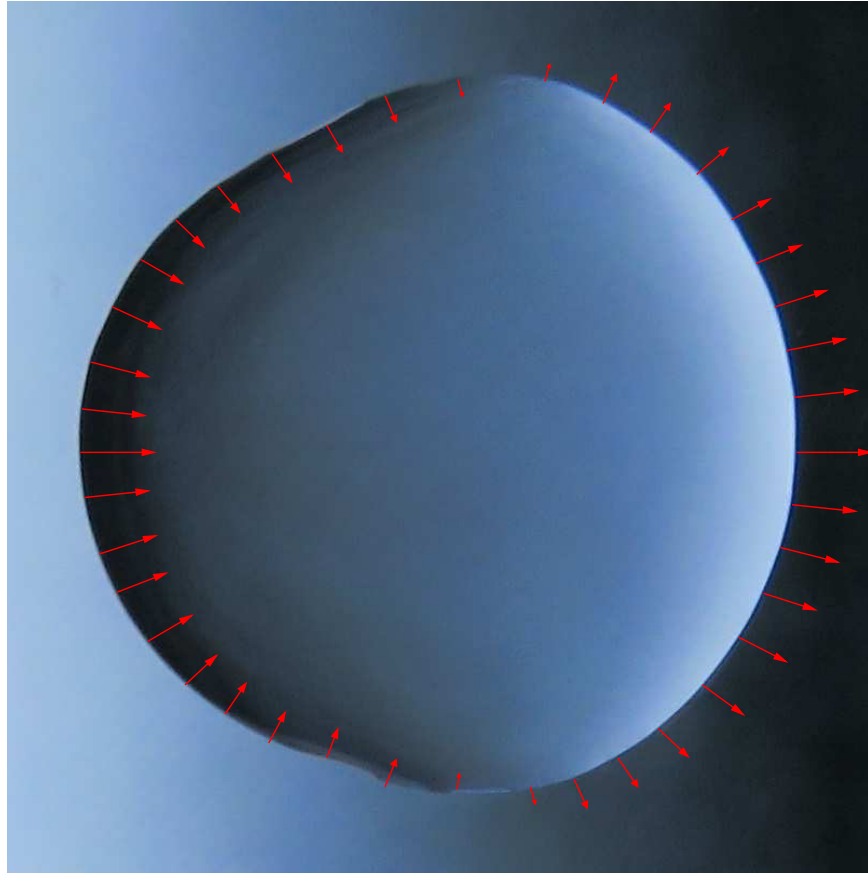


Figure 2: Schematic representation of the types of surfaces and shapes of triple line we used in this work. (a) Circular triple line (represented by a solid line) on a uniform surface; (b) circular triple line encircling a hydrophobic island (represented by the gray circle); (c) circular triple line on a hydrophobic surface; (d) circular triple line encircling a single-circle scratch (represented by a dashed line); (e) circular triple line encircling a double-circle scratch; (f) circular triple line encircling a triple-circle scratch; (g) triple line elongated along the direction perpendicular to the centrifugal force; (h) triple line elongated along the direction of the centrifugal force; (i) direction of the centrifugal force.



The lateral retention force is independent of contact area

Figure 3: Graphical abstract.